# A Hybrid Weight Function Approach for the Computation of Stress Intensity Factor in Elliptical and Semi-elliptical Cracks

B.K. Hachi [1], S. Rechak [2], Y. Belkacemi [2] and M. Haboussi [3]

[1] Departement of electromechanical, C.U.D., BP 1317 Djelfa 17000, ALGERIA
[2] LGMD, Departement of mechanical engineering  , E.N.P., BP 182 Harrach 16200, Algiers, ALGERIA
[3] LEMTA, Univ. de Nancy, 2 Ave forêt de Haye, BP 160, 54504, Nancy, FRANCE

## ABSTRACT

The use of the weight functions in fracture mechanics appears in the literature in a very increasing way in particular in the computation of the stress intensity factor (SIF). The difficulties of calculation of this significant parameter, which come from the analytical singularities present in its formulation, encourage the use of the methods using weight functions for both their simplicity and their effectiveness with respect to the other approximate methods.

This work consists on  the hybridization of two weight functions developed by Oore & Burns [1] and Krasowsky & al.[2] in order to model the elliptical cracks for the computation of the stress intensity factor (SIF) in mode I. The idea of hybridization consists in dividing the ellipse into two zones, then to use each one of them in the area where it is more efficient. The proportion between the two zones is determined by optimization of the relationship between the small one and the large axis of the ellipse.

Compared with the exact solution, the maximum error of the results obtained is of 2.4%, whereas, for those of Krasowsky & al.[2] and Oore & Burns[1], the maximum error is 6.3% and 17.4%, respectively, and this in the case of an elliptical crack uniformly charged in an infinite body. Our approach is tested on another practical example of an internal semi-elliptical crack in tubes.

In the absence of the exact solutions, the results found by our calculations are in strong correlation with those of other authors using various techniques (FEM for  [3]  & WFM for [2]).

The idea of hybridization thus really demonstrated its effectiveness like its flexibility in the computation of SIF for a variety of problems in fracture mechanics.

## 1- INTRODUCTION

The development of the weight functions in fracture mechanics started with the work of Bueckner [4] in 1970, based on the formulation by the Green's function, for a semi-infinite crack, in an infinite medium.

The investigation in the weight functions on the one hand and the evaluation of the energy balance formula of Rice [5] on the other hand, allowed the extension of the use of the weight functions by several authors such as Oore & Burns [1] and Bortmann & Al. [6]. In 1986, Gao & Rice [7] introduced the study of the stability of the fictitiously disturbed rectilinear form from which results the values of SIF along the crack front. Other investigations related especially to the fissure shape (ellipse, half of ellipse, quarter of ellipse, rectangle. . .), to the mode of rupture (mode I, II, III or mixed), and to the large domain of application (elastoplastic, elastodynamic, thermoelastic. . .), consequently succeeded. Among those works, one can chronologically mention,  Fett & al.[8] (1989), Vainshtok & al.[9] (1990), Dominguez & al.[10] (1992), Rooke & al.[11] (1994), Orynyak & al.[12] (1995), Zheng & al.[13] (1997), Kiciak & al.[14] (1998), Pommier & al.[15] (1999), Krasowsky & al.[2] (1999), Hachi & al.[16] (2003) and Christopher & al.[17] (2004). The principle of the weight function technique consists in employing one or more known solutions (known as of reference) of a particular case in order to find the solution for the general case. The reference solution generally comes from the analytical results (exact). But in some cases, the absence of such results obliges the authors, such as [12], [13], [14], [15] and [17], to use approximate solutions which could be the existing weight functions. The solution of the SIF in mode I using the weight function technique is given by the general form [12]:
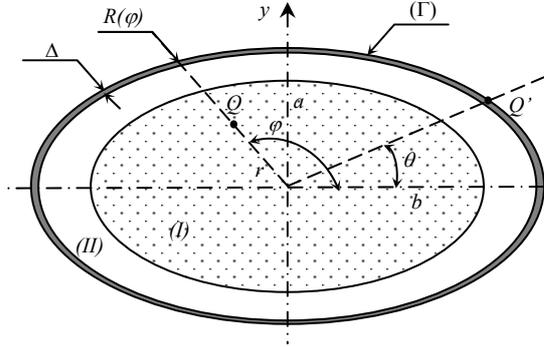
**Figure 1** Subdivision of the elliptical crack in two zones.
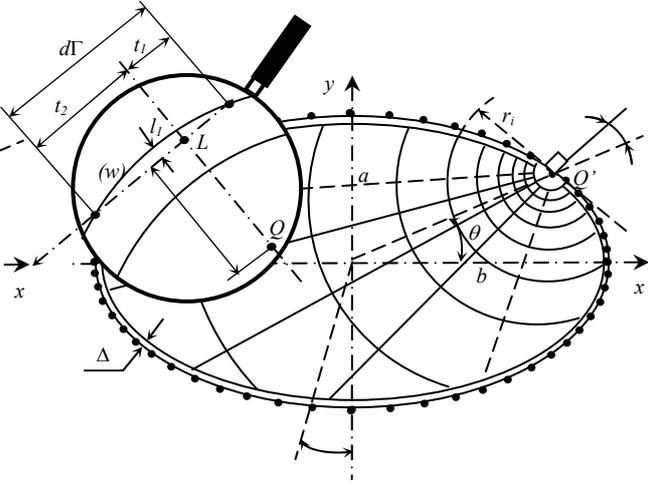
**Figure 2** Discretization of the fontour and the surface of the crack.

$$K_{IQ'} = \int\limits_{(S)} W_{QQ'} q(Q).dS \tag{1}$$

Where $K_{IQ'}$ is the stress intensity factor in mode I at *the (Q')* point of the crack front. $W_{QQ'}$ is the weight function related to the problem, and defined as $K_{IQ'}$ which is generated by a unit concentrated and symmetrical force applied to the arbitrary $Q$ point of the crack, and $q(Q)$ is the applied load at the Q point .

## 2- PRESENTATION OF THE HYBRIDIZATION TECHNIQUE

Our study is based on the hybridization of two weight functions deduced by the formulation of the Green's function. The first one is developed by Oore & Burns [1] to model any closed shape of a crack in an infinite body, including the elliptical cracks. Its expression is as follows:

$$W_{QQ'} = \frac{\sqrt{2}}{\pi . l^2_{QQ'} . \sqrt{\int\limits_\Gamma \frac{d\Gamma}{(\rho_Q)^2}}} \tag{2}$$

The second one is developed by Krasowski & Al. [2] to model elliptical cracks in an infinite body. Its expression is as follows:

$$W_{QQ'} = \frac{2.\prod^{1/4}(\theta)}{\sqrt{\pi a\left(1 - \frac{r^2(\varphi)}{R^2(\varphi)}\right)} . l^2_{QQ'} . \int\limits_\Gamma \frac{d\Gamma}{(\rho_Q)^2}} \tag{3}$$

with $r$ and $\varphi$ are the polar coordinates of an arbitrary point $Q$. $l_{QQ'}$ is the distance between the *(Q')* point and the arbitrary $Q$ point. $(\Gamma)$ is the curve of the ellipse (the crack front), and $\rho_Q$ is the distance between the $Q$ point and the elementary segment $d\Gamma$.

With $\prod(\theta) = (\sin^2 \theta + \alpha^4 \cos^2 \theta)/(\sin^2 \theta + \alpha^2 \cos^2 \theta)$ and $\alpha = a/b$.

The principle of hybridization is to divide the elliptical crack into two zones, an internal zone I and an external zone II (see figure 1), then to use each of the two weight functions in the area where it is more efficient.

The weight function of the eqn (3) is intended exclusively for the cracks of elliptical form. Nevertheless, it presents an additional singularity *(1-r/R)* $^{-1/2}$ compared to the eqn (2). This makes the eqn (3) less efficient in the vicinity of the crack front $(r \to R)$. This argument leads us to choose the weight function (3) for the elliptical zone I, and the weight function (2) for the external zone II, where the singularity *(1-r/R)* $^{-1/2}$ is very strong.

The hybridization verifies well the two geometrical limits of an elliptical crack $\alpha \to 0$ and $\alpha \to 1$, as long as the two functions (2) and (3) satisfy the two following conditions:

$$\bullet \; W_{QQ'} \underset{\alpha \to 1}{\to} W_{QQ'}(penny-shaped) = \frac{\sqrt{R^2 - r^2}}{\pi \sqrt{\pi R}\; l^2_{QQ'}} \tag{4}$$

Is the weight function of a penny-shaped crack in an infinite body [18].

$$\bullet \; W_{QQ'} \underset{\alpha \to 0}{\to} W_{QQ'}(straight) = \frac{\sqrt{2d}}{\pi \sqrt{\pi}\; l^2_{QQ'}} \tag{5}$$

Is the weight function of a straight line crack in a semi-infinite body [2]. $d$ is the shortest distance between the crack front and the arbitrary point $Q$.

The adequate proportion between the two zones is established by the optimization of the ratio $\alpha$ which allows us to conclude the following: the smaller is $\alpha$, the larger is zone I and the opposite is true. Thus, we adopted the following convention :

$$r/R \leq 1 - \alpha^2 \to W_{QQ'} = W_{QQ'} \; of \; eqn \; (3) \; and \; r/R > 1 - \alpha^2 \to W_{QQ'} = W_{QQ'} \; of \; eqn \; (2) \tag{6}$$

## 2. NUMERICAL PROCEDURE, MESHING AND SINGULARITIES

The solution in eqn (1) includes two integrals, a surface integral and a contour integral.

### 2.1 The surface integral

A treatment technique of singularity $1/l^2_{QQ'}$ in the eqn (1) is employed efficiently by Krasowsky & al.[2]. It consists in surrounding the $(Q')$ point by a small half-circle of $R_0$ radius on which the integral is evaluated analytically using eqn (5):

$$K_I^{S'} = \int_{(S')} \frac{\sqrt{2d}}{\pi \sqrt{\pi}} \frac{1}{l^2_{QQ'}} q(Q')dS' \approx 1.21703 \sqrt{R_0}\, q(Q') \tag{7}$$

The SIF will be in this case: $K_I^S = K_I^{S'} + K_I^{S''}$, $S$ is the surface of the ellipse, $S'$ is the surface of the half circle and $S''$ is the remaining surface. To minimize the error generated by the curvature in $(Q')$, one takes: $\qquad R_0 = (1/30 \sim 1/20)\min(R_i(Q'),a) \tag{8}$

$R_i$ is the radius of curvature of the crack front.

The meshing of $(S'')$ is generated by drawing concentric half-circles of $(Q')$ center and $R_0$, $r_0$, $r_1, r_2, r_3, ...$ radius which progressively increases then by draying half-lines of $(Q')$ origin dividing the half-plane of the ellipse into $n_j$ portions, approximately 60 (see figure 2). The integral on $(S'')$ will be calculated according to the meshing as shown in figure 2 by the ordinary numerical algorithms, such as the Gauss's algorithm.

### 2.2 The contour integral

When $Q$ is very close to the crack front, the integral $\int_{\Gamma} \left[ d\Gamma / (\rho_Q)^2 \right]$ becomes singular and its numerical calculation becomes delicate. To deal with this singularity we first ignore a very narrow band near the contour of thickness $\Delta$, where $\Delta = \gamma a$ and $\gamma = 1/300$, as shown in figure 1. The effective ellipse surface becomes: $\quad (x/b)^2 + (y/a)^2 \leq (1 - \Delta/R(\varphi))^2 \tag{9}$

To consider a thickness $\Delta$ as a variable[2] makes the automatic meshing very complex without gaining in the exactitude of calculation. The error is approximately estimated as $\left( \int_0^\gamma \sqrt{x}dx \middle/ \int_0^1 \sqrt{x}dx \right) \approx \gamma^{3/2}$ and $(2\gamma)^{3/2}$ for $\Delta(\varphi) = \gamma \cos(T(\varphi))\min(R_i(\varphi),a)$ and for $\Delta$ constant,

respectively. At any rate, the shortest distance between two successive arcs of circles must not be lower than the thickness Δ. Therefore, we must check the expression below:

$$\Delta = (r_{i+1} - r_i)_{\min} = r_0 - R_0 \tag{10}$$

and with the combination of the eqn (8), will give the progression of the $r_i$ radius as follows:

$$\nu = (r_{i+1} - r_i)/r_i = (r_0 - R_0)/R_0 \approx 1/15 \sim 1/10 \tag{11}$$

The numerical calculation of the contour integral requires the discretization of the crack front (Γ) with a finite number of points, delimiting straight segments of length $d\Gamma$ (figure2). The error of linearization of $d\Gamma$ is obtained by the use of Taylor's series expansion of $\sin(d\psi/2)$ in the vicinity of zero:

$$\varepsilon = (\hat{w} - \overline{w})/\hat{w} = (d\psi)^2/24 \approx (\pi/(2N))^2/24 \tag{12}$$

$N$ is the number of points on the quarter of contour (Γ), $d\psi$ is the angular opening of the $d\Gamma$. To uniformize the error $\varepsilon$ on all the contour (Γ), the opening $d\psi$ decreases with the reduction in the curvature radius. The angle $\psi$ of the $i^{th}$ point, must satisfy the following expression:

$$\psi(i) = \arctan\left[\alpha^2 \bigg/ \tan\left(\frac{\pi}{2} - i\frac{\pi}{2N}\right)\right] \tag{13}$$

To insure that the error $\varepsilon$ remains weak, Krasowsky & Al. [2] imposed the following condition (figure 2):

$$l_1(\varphi)/\Delta \le \mu \ with : \mu = 0.1 \div 0.2 \tag{14}$$

When coupling this condition with eqns (10), (11) and (12) we obtain the lower limit of $N$:

$$N \ge \pi \bigg/ \left(2\sqrt{8\mu\gamma}\right) \tag{15}$$

As long as the $Q$ point is far from ( Γ), the integral could be transformed into the summation:

$$\int_\Gamma \frac{d\Gamma}{(\rho_Q)^2} = \sum_{i=1}^{4N} \frac{(d\Gamma)_i}{\rho_{iQ}^2} \tag{16}$$

When $Q$ is very close to the $k^{th}$ segment, the integral must analytically be computed on this segment in order to avoid any risk of singularity. It is equal to (figure 2):

$$\int_{d\Gamma} \frac{dw}{\rho_Q^2} \approx \int_{t_1}^{t_2} \frac{dt}{t^2 + d^2} = \left|\frac{1}{d}\left(\arctan\frac{t_2}{d} - \arctan\frac{t_1}{d}\right)\right| \tag{17}$$

The eqn (16) thus becomes:

$$\int_\Gamma \frac{d\Gamma}{(\rho_Q)^2} = \sum_{i=1}^{k-1} \frac{d\Gamma}{\rho_{QL_i}^2} + \int_{d\Gamma} \frac{dw}{\rho_Q^2} + \sum_{k+1}^{4N} \frac{d\Gamma}{\rho_{QL_i}^2} \tag{18}$$

In order to justify the need for the use of the eqn (17), let us evaluate the error made by the eqn (16) when $Q$ is located on the border of the surface defined by the eqn (9). Let's for example, take the point $L$ (figure 2) to be in the middle of $d\Gamma$ $(t_1 = -t_2)$. For $d\Gamma = a(\pi/2N) = a\sqrt{8\mu\gamma}$ and $d = \Delta = a\gamma$, the integrals calculated by the eqn (16) and the eqn (17) are:

$$I_1 = \frac{d\Gamma}{d^2} = \frac{1}{a}\sqrt{\frac{8\mu}{\gamma^3}} \approx 5600a^{-1} \ and \ \ I_2 = \left|\frac{2}{a\gamma}\arctan\left(\sqrt{\frac{2\mu}{\gamma}}\right)\right| \approx 880a^{-1}, \text{ respectively.}$$

The error is obviously enormous (more than 600%!!!).

### 3. APPLICATIONS AND RESULTS
#### 3.1 Elliptical crack in an infinite body

A computer code, with graphic visualization of the meshing, named *HWFun* is established (figure 3). We calculate thus, the adimensional stress intensity factor $\overline{K}_I = K_I E(k) \bigg/ \left(\sqrt{\pi a}\Pi^{1/4}(\theta)\right)$, *E(k)* is the complete elliptical integral of the second kind where $k = \sqrt{1 - \alpha^2}$ for an elliptical crack in an

infinite body subjected to a uniform unit loading. The computation is carried out for various values of the $\alpha$ ratio and for various values of the reduced angle $\overline{\theta}$, with $\overline{\theta} = \arctan(\tan(\theta)/\alpha)$. The obtained results are compared with those of [1] and [2] and with the exact solution as well.

According to table I, the hybridization undoubtedly shows a clear improvement of the results compared to those of [1] and [2], and this for various values of $\alpha$ and $\overline{\theta}$. The maximum error of the results obtained is 2.4%, whereas, for those of Krasowsky & al.[2] and Oore & Burns[1], the maximum error is 6.3% and 17.4% respectively.

| $\alpha$ | $\overline{\theta}°$ | Chargement uniforme $q(Q) = 1$ | | | |
|---|---|---|---|---|---|
| | | $\overline{K}_I{}^{(exacte)}$ | $\overline{K}_I{}^{HWFun}$ | $\overline{K}_I{}^{[2]}$ | $\overline{K}_I{}^{[1]}$ |
| 1.0 | 0. | 1.00000 | 0.99761 | 1.00035 | 0.99761 |
| | 30. | 1.00000 | 0.99777 | 1.00035 | 0.99777 |
| | 60. | 1.00000 | 0.99780 | 1.00035 | 0.99780 |
| | 90. | 1.00000 | 0.99778 | 1.00035 | 0.99778 |
| 0.8 | 0. | 1.00000 | 1.00690 | 0.98523 | 1.01049 |
| | 30. | 1.00000 | 0.99934 | 0.99170 | 1.00133 |
| | 60. | 1.00000 | 0.99147 | 1.00573 | 0.98992 |
| | 90. | 1.00000 | 0.99090 | 1.01184 | 0.98732 |
| 0.6 | 0. | 1.00000 | 1.00657 | 0.96532 | 1.03307 |
| | 30. | 1.00000 | 0.99166 | 0.98550 | 1.00562 |
| | 60. | 1.00000 | 0.98845 | 1.00985 | 0.97917 |
| | 90. | 1.00000 | 0.99891 | 1.01390 | 0.97695 |
| 0.4 | 0. | 1.00000 | 0.99556 | 0.94460 | 1.07646 |
| | 30. | 1.00000 | **0.97587** | 0.98180 | 1.00893 |
| | 60. | 1.00000 | 0.99077 | 1.00540 | 0.96820 |
| | 90. | 1.00000 | 1.00858 | 1.02053 | 0.96726 |
| 0.2 | 0. | 1.00000 | 0.99070 | **0.93730** | **1.17447** |
| | 30. | 1.00000 | 0.98544 | 0.99690 | 1.00934 |
| | 60. | 1.00000 | 0.98421 | 1.00400 | 0.96464 |
| | 90. | 1.00000 | 0.99515 | 1.00400 | 0.96143 |
| 0.1 | 0. | 1.00000 | 1.00270 | - | - |
| | 30. | 1.00000 | 0.99945 | - | - |
| | 60. | 1.00000 | 0.98808 | - | - |
| | 90. | 1.00000 | 0.99726 | - | - |
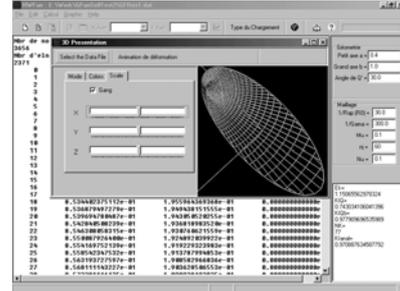


**Figure 3** Interface of HWFun Computer code

**Tableau I** Adimensional SIF for elliptical crack infinite body.

| $i$ | $\overline{\theta}°$ | $\alpha = 1.0$ | | | $\alpha = 0.4$ | | |
|---|---|---|---|---|---|---|---|
| | | $\overline{K}_I{}^{FEM[3]}$ | $\overline{K}_I{}^{HWFun}$ | $\overline{K}_I{}^{[2]}$ | $\overline{K}_I{}^{FEM[3]}$ | $\overline{K}_I{}^{HWFun}$ | $\overline{K}_I{}^{[2]}$ |
| 0 | 0. | 1.2190 | - | - | 1.4800 | - | - |
| | 90. | 1.0500 | - | - | 1.2170 | - | - |
| 1 | 0. | 0.2210 | 0.2368 | 0.2090 | 0.2780 | 0.2689 | 0.2500 |
| | 90. | 0.7290 | 0.7330 | 0.7360 | 0.7230 | 0.7160 | 0.7120 |
| 2 | 0. | 0.0850 | 0.0910 | 0.0830 | 0.1090 | 0.0983 | 0.0910 |
| | 90. | 0.5960 | 0.6068 | 0.6120 | 0.5490 | 0.5473 | 0.5550 |
| 3 | 0. | 0.0440 | 0.0456 | 0.0430 | 0.0570 | 0.0474 | 0.0450 |
| | 90. | 0.5150 | 0.5340 | 0.5380 | 0.4560 | 0.4608 | 0.4700 |

**Tableau II** Adimensional SIF pour semi-elliptical surface crack in tube

### 3.2 Internal semi-elliptical surface crack in tube

The theory of the thick tubes (Lamé's theory) shows that the longitudinal cracks located on the internal face of the tube are most dangerous. For this situation, we test our approach of hybridization, via the "Point Weight Function Method" (PWFM)[12]. The test is made on tubes of $e/R_{int} = 0.1$, where $e$ is the thickness of tube and $R_{int}$ is its internal raduis, for values of $\alpha=1.0$ and $\alpha=0.4$. The loading inside the crack has the form $p = (y/a)^i$ with $i \in \{1,2,3\}$. The reference solution[12] is for $p = (y/a)^0 = 1$. The results found by our computer code *HWFun* for $\theta = 0°$ and $\theta = 90°$ are grouped in table II along with those of [3] and [2]. Those results prove the utility and

the efficiency of our approach. Indeed, our results are in strong correlation with those of the references [3] and [2].

## CONCLUSION

For elastic and homogeneous bodies, a modelling of the elliptical and semi-elliptical cracks for the determination of the stress intensity factor in mode I is carried out. This is obtained by hybridization of the two weight functions developed by [1] and [2]. The results obtained show a clear reduction in the error. Tested on two practical applications, the present approach demonstrates its robustness as well as its reliability.

**References:**
[1] Oore M., Burns D.J., Transaction of the ASME Journal of pressure Vessel Technology, 102 N° 2, 202-211 (1980).
[2] Krasowsky A.J., Orynyak I.V. & Gienko A.Yu., Approximate Closed from Weight Function for an Elliptical Crack in an Infinite Body, Int. J. Fract., 99 (1-2), 117-130 (1999).
[3] Raju I.S. & Newman J.C.Jr., Stress-intensity factors for internal and external surface cracks in cylindrical vessels, Trans. of ASME J. Press. Vess. Tech., 104, 293-298 (1982).
[4] Bueckner H.F., A novel principle for the computation of stress intensity    factors, Z. Angew Meth., 50, 529-546 (1970).
[5] Rice J.R., Some remarks on elastic crack-tip stress fields, Int. J. Sol. Struct., 8, 751-758 (1972).
[6] Bortmann Y. & Banks-Sills L., An extended weight function method for 2D and 3D-problems, Journal of Applied Mechanics, 50, 907-909 (1983)
[7] Gao H. & Rice J.R., Shear stress intensity factors for planar crack with slightly curved front, Journal of Applied Mechanics, 53, 774-778 (1986).
[8] Fett T., Mattheck C. & Munz D., Approximate weight function for 2D and 3D-problems, Engineering Analysis with Boundary Elements, 6, 37-48 (1989).
[9] Vainshtok V.A. & Varfolomeyev I.V., International Journal of Fracture, 46, 1-24 (1990).
[10] Dominguez J. & Gallego F., Time domain boundary element method for dynamic stress intensity factor computations, Int. J. Num. Meth. Engng., 33, 635-647 (1992).
[11] Rooke D.P., & Aliabadi M.H., The use of fundamental fields to obtain weight functions for mixed-mode cracks, Int. J. Engng. Sci., 32, 155-166 (1994).
[12] Orynyak I.V. & Borodii M.V., Point weight function method application for semi-elliptical mode I cracks, International Journal of Fracture, 70, 117-124 (1995)
[13] Zheng X.J., Kiciak A. & Glinka G., Weight functions and stress intensity factors for internal surface semi-elliptical crack in thick-walled cylinder, Engng. Fract. Mech., 58 N° 3, 207-221 (1997)
[14] Kiciak A., Glinka G. & Eman M., Weight functions and stress intensity factors for corner quarter-elliptical crack in finite thickness plate subjected to in-plane loading, Engineering Fracture Mechanics, 60 N° 2, 221-238 (1998).
[15] Pommier S., Sakae C. & Murakami Y., An empirical stress intensity factor set of equations for a semi-elliptical crack in semi-infinite body subjected to a polynomial stress distribution, International Journal of Fatigue, 21, 243-251 (1999).
[16] Hachi B.K., Belkacemi Y., Rechak S. Computation of the stress intensity factor and stress analysis in 3D by using the Green's function in displacement discontinuity method, Revue de mécanique appliquée et théorique *(in French)*, Vol. 1 (5), 289-310 (2003).
[17] Christopher T., Sankarnarayanasamy K. & Rao B.N., Fracture behaviour of maraging steel tensile specimens and pressurized cylindrical vessels, Fatigue Fract. Engng. Mater. Struct., Vol. 27, 177-186 (2004).
[18] Guidera & Lardner R.W., Journal of Elasticity, 5 N° 1, 59-73, (1975).